proceedings

MDPI

Proceedings

Static and Fatigue Damage Characterization of Carbon/Epoxy Angle-Ply Laminates with the Use of Acoustic Emission and Online Microscopy †

Kalliopi-Artemi Kalteremidou [1,*], Eleni Tsangouri [1], Anghel Cernescu [1,2], Brendan R. Murray [1,2], Lincy Pyl [1], Dimitrios G. Aggelis [1] and Danny Van Hemelrijck [1]

[1] Department of Mechanics of Materials and Constructions, Vrije Universiteit Brussel (VUB), Pleinlaan 2, BE-1050 Brussels, Belgium; Eleni.Tsangouri@vub.be (E.T.); Anghel-Vasile.Cernescu@vub.be (A.C.); Brendan.Murray@vub.be (B.R.M.); Lincy.Pyl@vub.be (L.P.); Dimitrios.Aggelis@vub.be (D.G.A.); Danny.Van.Hemelrijck@vub.be (D.V.H.)

[2] SIM M3 Program, Technologiepark 935, B-9052 Zwijnaarde, Belgium

* Correspondence: Kalliopi-Artemi.Kalteremidou@vub.be; Tel.: +32-26-29-29-24

† Presented at the 18th International Conference on Experimental Mechanics, Brussels, Belgium, 1–5 July 2018.

Published: 14 May 2018

Abstract: In the current work, a combined non-destructive methodology is proposed in order to investigate the static and fatigue damage of carbon fiber reinforced epoxy composites. Flat angle-ply laminates are used in order to examine the influence of multiaxial stress states on the mechanical performance using different non-destructive techniques. Acoustic emission is combined with an online microscope and digital image correlation and this combination is used to comprehend the performance of composites with unequal stress states.

Keywords: carbon fiber reinforced composites; non-destructive techniques; acoustic emission; fatigue; damage investigation; multiaxiality

1. Introduction

The damage and failure mechanisms of composite materials are more complex than that of metals. It has been observed that composites, especially under fatigue, exhibit a gradual accumulation of damage of various types. Damage usually occurs through matrix cracking, fiber-matrix interfacial debonding, delamination and fiber failure. It has been proven that matrix cracks initiate even from the first cycles of the fatigue life and then propagate throughout the laminate width until the sudden failure of the material [1]. Moreover, fatigue life of composite materials is characterized by a gradual degradation of their mechanical properties (stiffness and strength) which begins even from the very early stages of their life. This means that understanding the evolution of the damage mechanisms throughout the fatigue life is important as this is responsible for the mechanical degradation.

Another significant issue related to the fatigue behavior of composite materials which has gained more research interest is that the damage sequence strongly depends on the multiaxial stress states that develop in the separate layers of the laminate [2]. Even on flat specimens with different stacking sequence, global unidirectional loading creates different local multiaxial stress states on a ply level due to the anisotropy that characterizes composite materials [3,4]. Therefore, the possibility of using flat specimens with different lay-ups to identify how damage progresses under different multiaxial loading conditions is investigated in this research.

Various methods have been proposed for the identification of damage on Glass Fiber Reinforced Polymers (GFRPs) [5,6], but there is still not a straightforward method identified for measuring the

damage on Carbon Fiber Reinforced Polymers (CFRPs). For this reason, in this study, a combined Non Destructive Testing (NDT) methodology is proposed to qualitatively and quantitatively estimate the damage of CFRPs. Therefore, flat angle-ply laminates were loaded under static and fatigue conditions and their response was continuously monitored using an online microscope, Acoustic Emission (AE), which is effectively used in literature for the damage investigation of composites [7,8], and Digital Image Correlation (DIC). The aim of this research is the establishment of a NDT methodology in order to physically estimate and measure the static and fatigue damage and to correlate its sequence with the different multiaxial stress states acting on flat CFRP specimens. Moreover, characterization of the different AE responses related to dissimilar multiaxial stress states and investigating the potential of using AE as a predictive tool for damage identification under different stress states on CFRP specimens is a significant target of this research.

2. Materials and Equipment

In order to study the response of CFRP composites under dissimilar multiaxial stress states, two angle-ply laminates, namely $[0°/30°]_{2s}$ and $[0°/60°]_{2s}$, manufactured by Mitsubishi Chemical Corporation, were used in this research. Specimens were cut with dimensions according to ASTM D3039 and they were tabbed for a length of 50 mm on both sides using the same CFRP material.

The choice of the lay-up of the different laminates was made in such a way that different biaxiality ratios λ (i.e., $\lambda_{12} = \sigma_6/\sigma_2$, where σ_2 is the transverse stress and σ_6 is the in-plane shear stress in the material's coordinate system) are developed in the separate layers of the laminate. Since shear is expected to be one of the most detrimental factors in the fatigue response of composites, significant attention was given on the corresponding σ_6 stress component.

Fatigue tests were performed at load levels determined from the appearance of damage in preliminary static tests. All tests were performed on a MTS servo-hydraulic machine with a load cell of 100 kN capacity. The static tests were performed in displacement control with a rate of 1 mm/min. The fatigue tests were performed in a load controlled configuration at a frequency of 3 Hz, using three different percentages of the ultimate strength as the maximum fatigue stress (70%, 80% and 90%) and one R-ratio ($R = \sigma_{min}/\sigma_{max}$) (0.1). At least 3 repetitions for each test case were performed.

Regarding the NDT set-up, first a Leica microscope was mounted on the frame of the MTS system. This allowed for the monitoring of the through-thickness damage of the material in specific steps during testing. The acoustic activity during the tests was measured using an eight-channel DiSP system by Physical Acoustics. Two piezoelectric transducers (Pico) with a broadband response and maximum sensitivity at 450 kHz were mounted on the specimen using vaseline. A commonly used 35 dB threshold was applied to filter out the noise of the mechanical system (7). The strains during testing were measured using a 50 mm extensometer. At the same time, a DIC system (VIC-3D by Correlated Solutions with two Stingray Cameras of 5 MP and 23 mm lenses) was used in order to obtain the full-field strain maps during testing through triangulation of the two cameras.

The combination of the above mentioned NDTs was used in order to understand the influence of the multiaxiality and, most importantly, to determine the influence of the shear acting on a lamina level on the static and fatigue damage process and the mechanical performance of the material.

3. Results and Discussion

Before examining the fatigue behavior of the angle-ply laminates, a sufficient understanding of the static response is important. In Table 1, the mechanical properties of the two tested laminates acquired by the quasi-static tests are presented.

Looking at Table 1, it is worth mentioning that both laminates present a very similar mechanical behavior under quasi-static conditions. The $[0°/30°]_{2s}$ laminates result in a 4.1% gain in ultimate strength and a 5.2% gain in stiffness compared to the $[0°/60°]_{2s}$ laminates due to the fibers in their off-axis layers which are less inclined with respect to the loading direction than in the $[0°/60°]_{2s}$ laminates. This is obviously expected from classic laminate theory since the fibers in the 30° layers can carry more load than those in the 60° layers.

Table 1. Mechanical properties of the off-axis laminates acquired from the quasi-static tests.

	Ultimate Strength [MPa]	E-Modulus [GPa]	Strain to Failure [%]
$[0°/30°]_{2s}$	1374.57	78.15	1.57
$[0°/60°]_{2s}$	1317.53	74.11	1.71

What changes in the static performance between the two laminates is the damage sequence. Concerning the $[0°/30°]_{2s}$ laminates, until 70% of the ultimate load, no damage was observed with the microscope. At this load, an initial splitting of the fibers on the outer 0° layer was recorded and at around 75% an initial delamination between this outer 0° and the adjacent 30° layer was evident. At the same load, splitting of the fibers on the other outer 0° layer was noticed. At this stage, only some random matrix cracks, very limited in their number, were recorded in the middle thick 30° layer. Between 75% and 85% load (Figure 1), the second outer 0° layer was also delaminated from its adjacent 30° layer and delamination growth at both sides was observed. At 85% load, multiple cracks on one of the thin 30° layers were recorded and a third delamination between this and the inner 0° layer was visible. The growth of all these delaminations resulted in the final failure of the material.

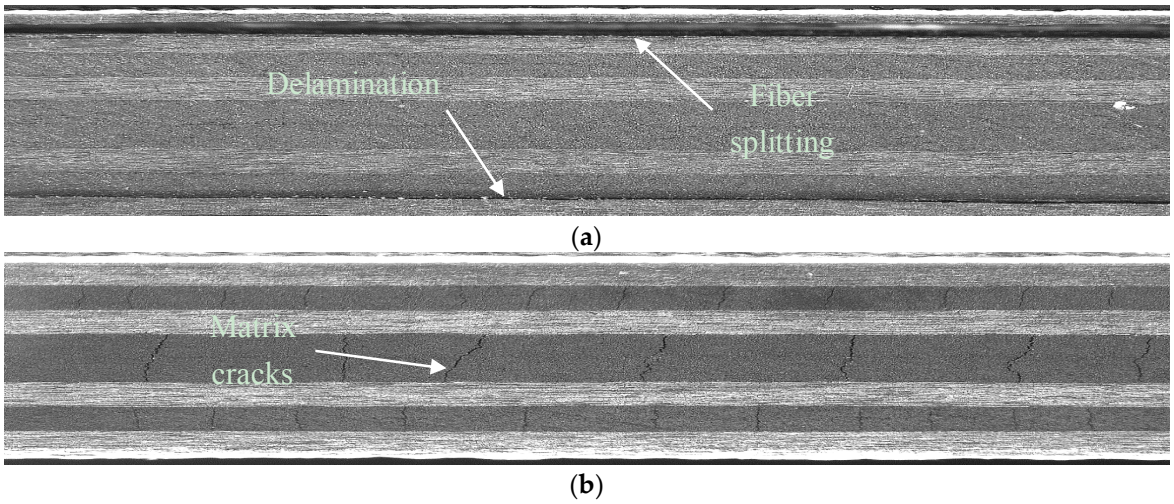

Figure 1. Damaged state at a load equal to 75% of the ultimate one for (**a**) $[0°/30°]_{2s}$ laminates and (**b**) $[0°/60°]_{2s}$ laminates.

For the $[0°/60°]_{2s}$ laminates, the damage sequence was different. Even from a load equal to 45% of the ultimate one, some random matrix cracks both in the thin and in the thick 60° layers were monitored. At a 60% load, multiple matrix cracks were monitored in all off-axis layers with a higher crack density for the thinner off-axis layers. Until 85% load, an increase in the matrix cracks was monitored in all off-axis layers (Figure 1) and only at a 90% load level an initial delamination between the outer 0^o layer and the adjacent 60° layer was recorded which led to the final failure.

In Figure 1, the damaged state of the two off-axis laminates at 75% load is presented, in which it is obvious that in the $[0°/60°]_{2s}$ laminates matrix cracking is the most pronounced damage mode whereas in the $[0°/30°]_{2s}$ almost no matrix cracks appear and delamination is the main damage mode. This can be explained and correlated with the different stress states acting on a lamina level at the two laminates. In the $[0°/30°]_{2s}$ laminates, the $\lambda_{12} = \sigma_6/\sigma_2$ ratio equals to 2.02 while in the $[0°/60°]_{2s}$ laminates it equals to 0.64 showing that the first laminates are subject to local shear damage which leads to delaminations whereas in the second one the matrix cracks are more pronounced.

In Figure 2, the total AE for the two laminates is shown. The first remark is that during the static tests of the $[0°/30°]_{2s}$ laminates, more AE events are recorded in comparison to the $[0°/60°]_{2s}$ ones. Moreover, the first laminates exhibit an exponential increase of the AE events, whereas the second ones do not. For the $[0°/60°]_{2s}$ laminates, no AE activity is observed until a load equal to 35% of the ultimate one. At this level, AE events are recorded related to initial matrix microcracking that was

not visible with the microscope and at a 45% load, an increase in the number of the AE events is evident, which coincides with the stage at which matrix cracks were monitored with the microscope. This increase continues until a 90% load and after this a sudden increase in the AE events occurs, coinciding with the appearance of delamination. On the other hand, the $[0°/30°]_{2s}$ laminates show AE activity with different features earlier than the $[0°/60°]_{2s}$ laminates even if no damage is monitored with the microscope. Most of this activity can be attributed to local shear debondings appearing quite early in the static test and increasing exponentially until the final failure with a high increase in the AE activity after a load of 70% at which point the first visible damage occurs and shear debondings lead to delaminations.

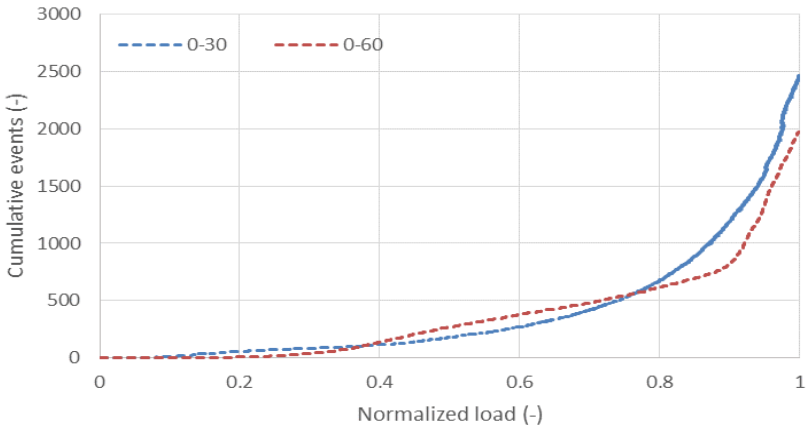

Figure 2. Total AE events recorded for the two laminates during the static tests.

A further features analysis of the AE events can allow the characterization of the AE signals of the two laminates, since the AE difference is not only quantitative but also qualitative. The signals recorded for the two laminates will have different features related to their damage, which is shear dominated for the $[0°/30°]_{2s}$ whereas it is matrix cracking dominated for the $[0°/60°]_{2s}$ laminates. Therefore, identification of signals related to specific damage mechanisms will be possible. The above also proves that AE can be efficiently used to predict microscale damage earlier than any visible damage is monitored. For the $[0°/30°]_{2s}$, damage events are monitored from AE much earlier than any visible damage and for the $[0°/60°]_{2s}$ laminates, the initiation of matrix cracks is recorded already from a 35% load in comparison to the 45% load that they are captured by the microscope.

The influence of the different stress states of the two laminates was also studied under fatigue and the effect of the high shear stresses acting on the off-axis plies of the $[0°/30°]_{2s}$ laminates was evident. The choice of the load levels was made in such a way that high loads are introduced in the material related to the appearance of damage in the static tests.

The initial remarkable finding is that for 70% and 80% of load, the $[0°/30°]_{2s}$ laminates lead to significantly lower fatigue lives than the $[0°/60°]_{2s}$ laminates, with a 43% reduction for 80% maximum load and a 22% reduction for 70% maximum load. Only when the applied load reaches 90% of the ultimate load, the $[0°/30°]_{2s}$ laminates exhibit 35% higher fatigue life in comparison to the $[0^o/60^o]_{2s}$ laminates. The differences in the fatigue lives can be also shown by the damage process.

In Figure 3, a characteristic example of the damaged state of the laminates after 10 and 200 fatigue cycles for a 70% maximum load fatigue test is shown. In the first stage, only a few limited matrix cracks are evident for the $[0°/30°]_{2s}$ laminates and no other damage mode, while multiple matrix cracks have already appeared for the $[0°/60°]_{2s}$ laminates. However, after 200 fatigue cycles, an initial delamination in a length of 2.5 cm is noticed for the $[0°/30°]_{2s}$ laminates while in the $[0°/60°]_{2s}$ laminates a small increase in the matrix cracks density only for the thin 60^o laminates is shown. After 1000 cycles, the delamination has increased in 4 cm for the $[0°/30°]_{2s}$ laminates while already a second delamination has initiated. On the other hand, the $[0°/60°]_{2s}$ laminates are delaminated only after 50,000 cycles with the delamination growth progressing very slowly and the matrix cracking coming to a saturation already after 1000 cycles.

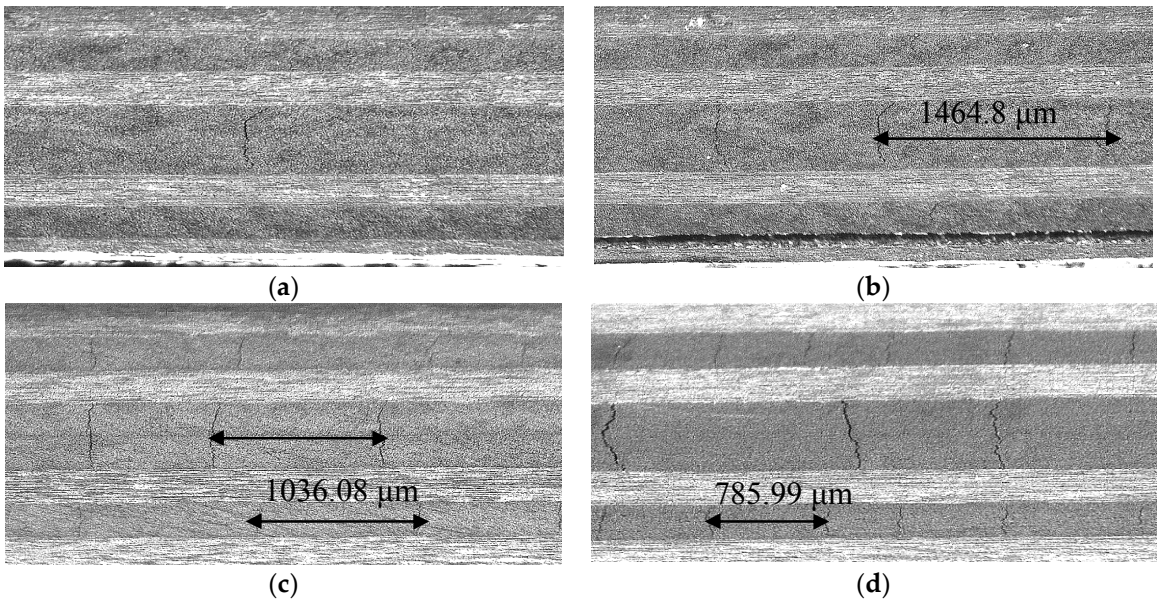

Figure 3. Fatigue damage state at 70% maximum load for $[0°/30°]_{2s}$ laminates after (**a**) 10 cycles and (**b**) 200 cycles and for $[0°/60°]_{2s}$ laminates after (**c**) 10 cycles and (**d**) 200 cycles.

Similar remarks are found for the 80% test as well, with the only difference being that the damage progresses more rapidly than for the 70% test. The basic difference occurs for a 90% test, at which both laminates are delaminated even in the first 50 cycles of fatigue, but in this case the highest σ_1 component of the $[0°/30°]_{2s}$ laminates acts as a supporting tool to carry the load for some more fatigue cycles, increasing the fatigue life for 35% in comparison to the $[0°/60°]_{2s}$ laminates.

Taking into consideration the mechanical response of the two laminates, the damaged state can be also shown by their stiffness degradation. A characteristic example is that for 80% fatigue load level, the $[0°/30°]_{2s}$ laminates are characterized by a rapid decrease of the stiffness already from the first 500 fatigue cycles and then a more stable but continuous decrease appears due to the developing delaminations and the forming of matrix cracks reaching a 24% stiffness loss until the end of the fatigue life. On the other hand, the $[0°/60°]_{2s}$ laminates have only a 13% stiffness loss until the end of their fatigue life giving a very stable reduction throughout the whole fatigue life.

The AE monitored for both laminates can also give an estimation of the total fatigue damage induced in the laminates. As shown in Figure 4, for a fatigue test of 70% maximum load for both laminates, significant AE is recorded in the initiation of the fatigue life but for the $[0°/30°]_{2s}$ laminates it continues increasing more intensely due to the continuous shear debondings and the appearance and increase of new delaminations whereas for the $[0°/60°]_{2s}$ laminates it evolves in a more stable manner. In both cases, a sudden increase in the AE activity appears towards the end of the fatigue life. The total number of AE events recorded for the two laminates also gives a good representation of the accumulated damage which is more pronounced for the $[0°/30°]_{2s}$ laminates.

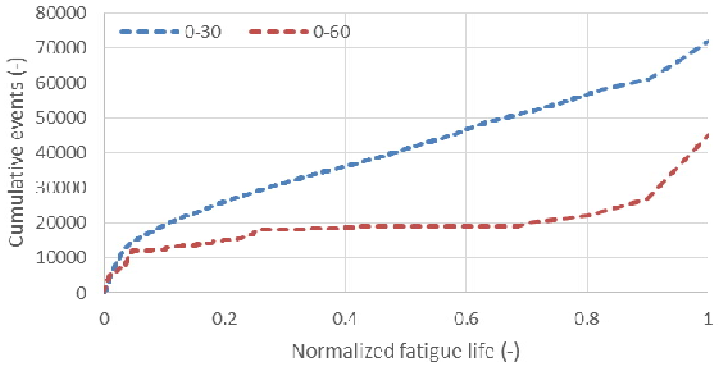

Figure 4. Total AE events recorded for the two laminates during the fatigue life for a 70% test.

4. Conclusions

In the current study, the influence of the different multiaxial stress states and, more significantly, the influence of the shear component on the static and fatigue behavior of two angle-ply laminates was investigated. Under static loads, the shear influence was not shown in the mechanical response but it influenced the damage progress. Under fatigue loads, shear was proven to be detrimental leading to smaller fatigue life and higher stiffness degradation; something that was also shown by the damage sequence. Higher shear components have also shown a greater possibility for the appearance of shear debondings which lead to the initiation of delaminations. Online microscopy was effectively used to monitor the static and fatigue damage and AE proved to be a reliable tool for the damage prediction and identification of different mechanisms.

Author Contributions: K.A.K., L.P. and D.V.H. conceived and designed the experiments; K.A.K. performed the experiments, collected, analyzed and interpreted the data; E.T. and D.G.A. contributed in the analysis and interpretation of AE data; A.C. and B.R.M. contributed in the establishment of the experimental set-up.

Acknowledgments: The work leading to this publication has been funded by the SBO project "M3Strength", which fits in the MacroModelMat (M3) research program funded by SIM (Strategic Initiative Materials in Flanders) and VLAIO (Flanders Innovation & Entrepreneurship Agency). The authors gratefully acknowledge the material suppliers Mitsubishi Chemical Corporation and Honda R&D Co., Ltd. The authors would also like to thank the financial support of the Fonds Wetenschappelijk Onderzoek (FWO) research funding program "Multi-scale modelling and characterization of fatigue damage in unidirectionally reinforced polymer composites under multiaxial and variable-amplitude loading".

Conflicts of Interest: The authors declare no conflict of interest. The founding sponsors had no role in the design of the study; in the collection, analyses, or interpretation of data; in the writing of the manuscript. The consortium of people involved in the M3 program and the material suppliers have accepted the publication of the results.

References

1. Reifsnider, K.A.; Talug, A. Analysis of fatigue damage in composite laminates. *Int. J. Fatigue* **1980**, *2*, 3–11.
2. Weng, J.; Wen, W.; Zhang, H. Multiaxial fatigue life prediction of composite laminates. *Chin. J. Aeronaut.* **2017**, *30*, 1012–1020.
3. Kalteremidou, K.A.; Fonteyn, S.; Carrella-Payan, D.; Pyl, L.; Van Hemelrijck, D. Experimental investigation of the fatigue behaviour of off-axis CFRP laminates using Non Destructive Techniques. In Proceedings of the 21st International Conference on Composite Materials, Xi'an, China, 20–25 August 2017.
4. Sevenois, R.D.B.; Garoz, D.; Gilabert, F.A.; Spronk, S.W.F.; Van Paepegem, W. Microscale based prediction of matrix crack initiation in UD composite plies subjected to multiaxial fatigue for all stress ratios and load levels. *Compos. Sci. Technol.* **2017**, *142*, 124–138.
5. Movahedi-Rad, A.V.; Keller, T.; Vassilopoulos, A.P. Fatigue damage in angle-ply GFRP laminates under tension-tension fatigue. *Int. J. Fatigue* **2018**, *109*, 60–69.
6. Quaresimin, M.; Carraro, P.A. Damage initiation and evolution in glass/epoxy tubes subjected to combined tension-torsion fatigue loading. *Int. J. Fatigue* **2014**, *63*, 25–35.
7. Godin, N.; Huguet, S.; Gaertner, R.; Salmon, L. Clustering of acoustic emission signals collected during tensile tests on unidirectional glass/polyester composite using supervised and unsupervised classifiers. *NDT E Int.* **2004**, *37*, 253–264.
8. Aggelis, D.G.; Barkoula, N.M.; Matikas, T.E.; Paipetis, S.A. Acoustic emission monitoring of degradation of cross ply laminates. *J. Acoust. Soc. Am.* **2010**, *127*, 246–251.